



University of Groningen

Synthesis and Enantiomeric Separation of a Novel Spiroketal Derivative

Fuggetta, Maria Pia; De Mico, Antonella; Cottarelli, Andrea; Morelli, Franco; Zonfrillo, Manuela; Ulgheri, Fausta; Peluso, Paola; Mannu, Alberto; Deligia, Francesco; Marchetti, Mauro

Published in:
Journal of Medicinal Chemistry

DOI:
[10.1021/acs.jmedchem.6b01046](https://doi.org/10.1021/acs.jmedchem.6b01046)

IMPORTANT NOTE: You are advised to consult the publisher's version (publisher's PDF) if you wish to cite from it. Please check the document version below.

Document Version
Final author's version (accepted by publisher, after peer review)

Publication date:
2016

[Link to publication in University of Groningen/UMCG research database](#)

Citation for published version (APA):

Fuggetta, M. P., De Mico, A., Cottarelli, A., Morelli, F., Zonfrillo, M., Ulgheri, F., Peluso, P., Mannu, A., Deligia, F., Marchetti, M., Roviello, G., Reyes Romero, A., Dömling, A., & Spanu, P. (2016). Synthesis and Enantiomeric Separation of a Novel Spiroketal Derivative: A Potent Human Telomerase Inhibitor with High in Vitro Anticancer Activity. *Journal of Medicinal Chemistry*, 59(19), 9140-9149. <https://doi.org/10.1021/acs.jmedchem.6b01046>

Copyright

Other than for strictly personal use, it is not permitted to download or to forward/distribute the text or part of it without the consent of the author(s) and/or copyright holder(s), unless the work is under an open content license (like Creative Commons).

Take-down policy

If you believe that this document breaches copyright please contact us providing details, and we will remove access to the work immediately and investigate your claim.

Downloaded from the University of Groningen/UMCG research database (Pure): <http://www.rug.nl/research/portal>. For technical reasons the number of authors shown on this cover page is limited to 10 maximum.

Synthesis and Enantiomeric Separation of a Novel Spiroketal derivative: A Potent Human Telomerase Inhibitor with High *In Vitro* Anticancer Activity

Maria Pia Fuggetta,^{†} Antonella De Mico,[‡] Andrea Cottarelli,[†] Franco Morelli,[§] Manuela Zonfrillo,[†] Fausta Ulgheri,[⊥] Paola Peluso,[⊥] Alberto Mannu,[⊥] Francesco Deligia,[⊥] Mauro Marchetti,[⊥] Giovanni Roviello,[#] Atilio Reyes Romero,[∇] Alexander Dömling,[∇] Pietro Spanu^{*⊥}*

[†] Istituto di Farmacologia Traslazionale - Consiglio Nazionale delle Ricerche, Via Fosso del Cavaliere, 00133 Roma, Italy

[‡] Istituto di Biologia e Patologia Molecolare - Consiglio Nazionale delle Ricerche, Piazzale Aldo Moro 5, 00185 Roma Italy

[§] Istituto di Genetica e Biofisica - Consiglio Nazionale delle Ricerche –Via Pietro Castellino 111 - 80131 Napoli, Italy

[⊥] Istituto di Chimica Biomolecolare - Consiglio Nazionale delle Ricerche, Trav. La Crucca 3, 07100 Sassari, Italy

[#]Istituto di Biostrutture e Bioimmagini - Consiglio Nazionale delle Ricerche, Via Mezzocannone

16, 80134 Naples, Italy

[∇]University of Groningen - Department of Drug Design - School of Pharmacy Antonius

Deusinglaan 1 Postbus 196 - 9700 AD Groningen - The Netherlands

KEYWORDS: Spiroketal, anticancer, apoptosis, telomerase.

ABSTRACT: The synthesis, the enantiomeric separation and the characterization of new simple spiroketal derivatives has been performed. The synthesised compounds have shown a very high anticancer activity. Cell proliferation assay showed that they induce a remarkable inhibition of cell proliferation in all cell lines treated, depending on culture time and concentration. The compounds have also shown a potent nanomolar human Telomerase inhibition activity and apoptosis induction. CD melting experiments demonstrate that spiroketal does not affect the G-quadruplex (G4) thermal stability. Docking studies showed that telomerase inhibition could be determined by a spiroketal interaction with the telomerase enzyme.

INTRODUCTION

Numerous complex natural products containing spiroketals framework have been isolated over the years from marine or terrestrial sources and have shown a wide range of important biological activities.^{1,2} Among them, the spongistatins **1** are a family of marine macrolides that display remarkable antitumor activity,³ integramycin **2** is an HIV-1 integrase inhibitor,⁴ reveromycins **3** are polyketide type antibiotics inhibitors of mitogenic epidermal growth factor (EGF) activity,⁵⁻⁷ tautomycin **4** and okadaic acid **5** are protein phosphatase inhibitors,⁸⁻¹⁰ spirofungin A **6** selectively inhibits the activity of isoleucyl-tRNA synthetase and displays antiproliferative activity of cancer cells,¹¹ and the rubromycins that exhibit an array of antimicrobial activity, cytotoxicity and potent ability to inhibit human telomerase (Figure 1).¹²⁻¹⁶

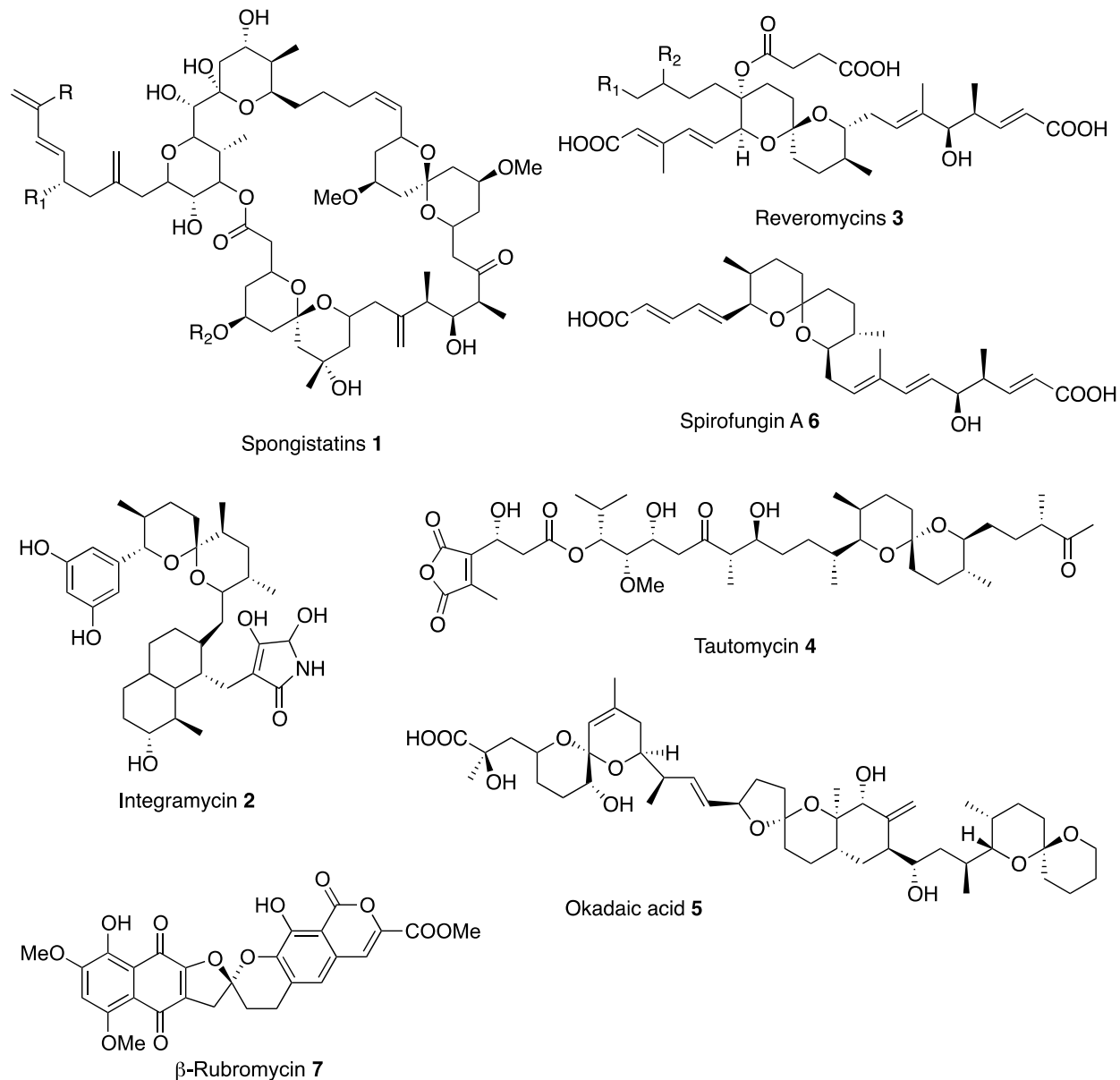


Figure 1. Biologically active naturally occurring spiroketals

Many groups started to investigate the possibility to reduce the complexity of spiroketal natural products while preserving their biological activity by focusing on the role of the spiroketal core on the biological activity of their natural models.¹⁷⁻¹⁹

So, the essential role of rubromycins spiroketal subunit for telomerase inhibition was demonstrated,¹² and natural inspired spiroketals **8**, **9** and **10** were synthesized showing interesting biological activity often retained from their parent natural products, while more recently, the simple spiroketal metabolite dinemasone A **11** was isolated from the fungus *Dinemasporium strigosum* and showed anti-microbial activity (Figure 2).²⁰⁻²³

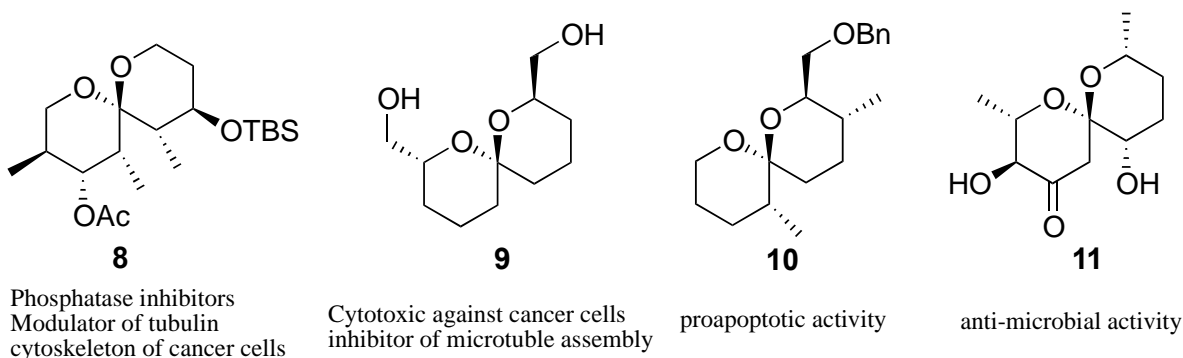


Figure 2. Biologically active simple spiroketals.

These results clearly demonstrate that simple spiroketals inspired to natural bioactive products can be privileged scaffolds for new lead compounds endowed with interesting biological activity.

Recently, some of us have synthesized a new structurally simplified spiroketal **12** that has shown potent antitumor activity against tumor cells of various nature and histotype (Figure 3).²⁴

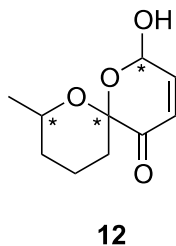


Figure 3. Structure of the new biologically active simple spiroketal

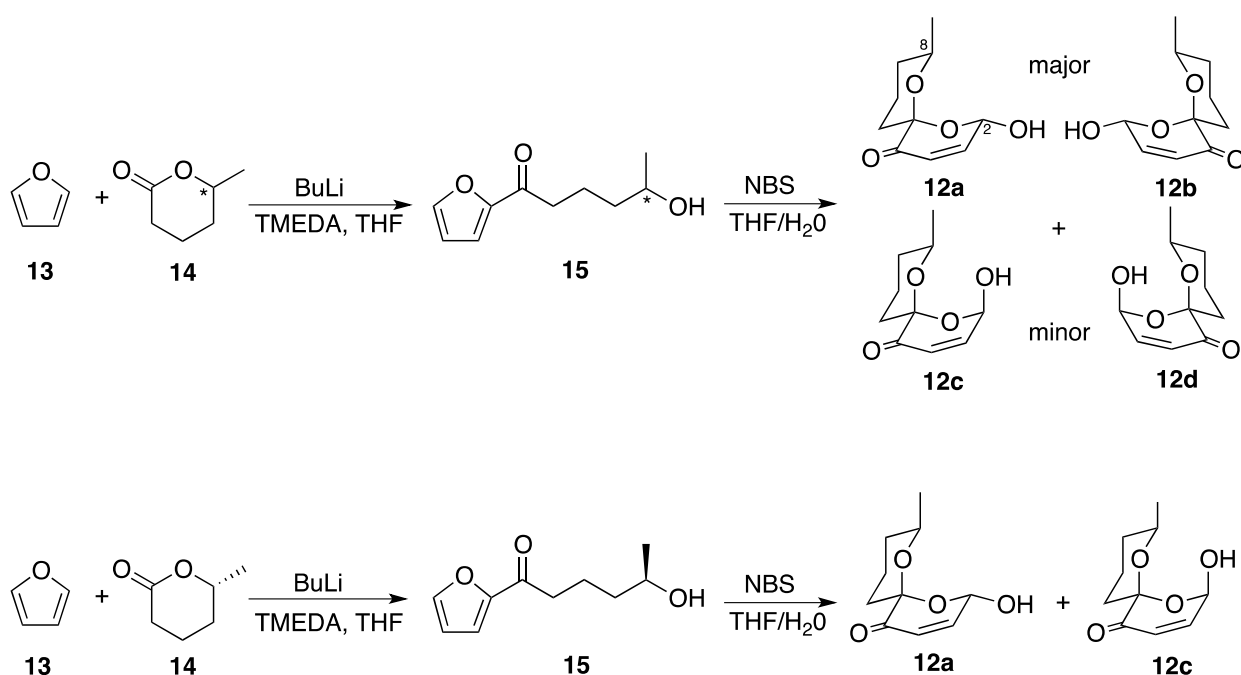
The simple spiroketalic structure of this compound is equipped with different stereocentres and its synthesis afforded a stereoisomeric mixture of the spiroketal **12** that as such was initially submitted to biological assay. Intrigued by the potent antitumor activity of the stereoisomeric mixture we decided to investigate the activity of the enantiomerically pure spiroketals. Here we describe the synthesis and the characterization of the stereoisomeric mixture of the spiroketal **12**, their stereoisomeric separation and the biological evaluation of the stereoisomeric mixture and the enantiomerically pure spiroketals. On the basis of docking and circular dichroism (CD) studies we highlighted that spiroketals induced telomerase inhibition could be determined by a spiroketal interaction with the telomerase enzyme rather than by a G-quadruplex (G4) stabilization mechanism.

RESULTS AND DISCUSSION

Chemistry.

The synthesis of the spiroketal derivative **12** has been performed via an oxidation-rearrangement of 2-furyl ketone **15** readily available by reaction of furyllithium with δ -hexalactone **14** as shown in Scheme 1.^{25,26} Starting from the racemic δ -hexalactone **14**, only two spiroketal diastereomers in 3:1 isomers ratio were detected via NMR, each consisting of a racemic mixture. The stereoisomers detected in the reaction mixture were supposed to have the configurations shown in Scheme 1 for compounds **12a,b** [(2*S*,6*S*,8*R*) and (2*R*,6*R*,8*S*)] and **12c,d** [(2*R*,6*S*,8*R*) and (2*S*,6*R*,8*S*)] because they are the only stereoisomers favoured from two anomeric effects derived from the axial-axial arrangement of the spiro C-O bonds.^{25,26,27} The configuration of the major diastereomers **12a,b** was supported by the observation of a Nuclear Overhauser Enhancement between the C-2 hydrogen and the C-8 hydrogen. As previously reported on similar spiroketals, the minor diastereomers

12c,d were assigned as the thermodynamically less stable corresponding C-2 epimers of **12a,b**. On the basis of the positive results of the biological tests performed on the mixture of stereoisomers **12a-d** (*see below*) the separation of the single stereoisomers was then performed by using chiral HPLC in order to test their individual biological activity. Finally in order to confirm the absolute configuration of the recovered stereoisomers, we carried out the synthesis of the spiroketal mixture of **12a** and **12c** starting from the enantiopure (*R*)- δ -hexalactone **14** (Scheme 1).



Scheme 1. Synthesis of spiroketal stereoisomers starting from racemic and enantiopure (*R*)- δ -hexalactone **14**

Chiral HPLC of the stereoisomers mixture of **12a-d**

With the aim to have at disposal milligram amounts of pure enantiomers for biological tests, the enantioseparability of the mixture containing the stereoisomers **12a-d** was investigated on two polysaccharide-based chiral columns (Chiralcel OD-H and Chiralpak IA) by using hex/IPA 95:5

as mobile phase (MP) at *FR* 0.8 ml/min. Four separated peaks were observed on both columns (Table 1). In general, the best column/MP chromatographic system can be selected as a suitable compromise between a high enough enantioselectivity value, a baseline resolution ($R_s \geq 1.5$) and a run-time as short as possible to complete the analysis. On this basis, Chiralcel OD-H was chosen for the multimilligram recovery of the stereoisomers. Indeed, despite baseline resolution was only achieved on Chiralpak IA (Figure 4), shorter elution times were obtained on Chiralcel OD-H, allowing to recover the enantiomers **12a** and **12b** within 15 min.

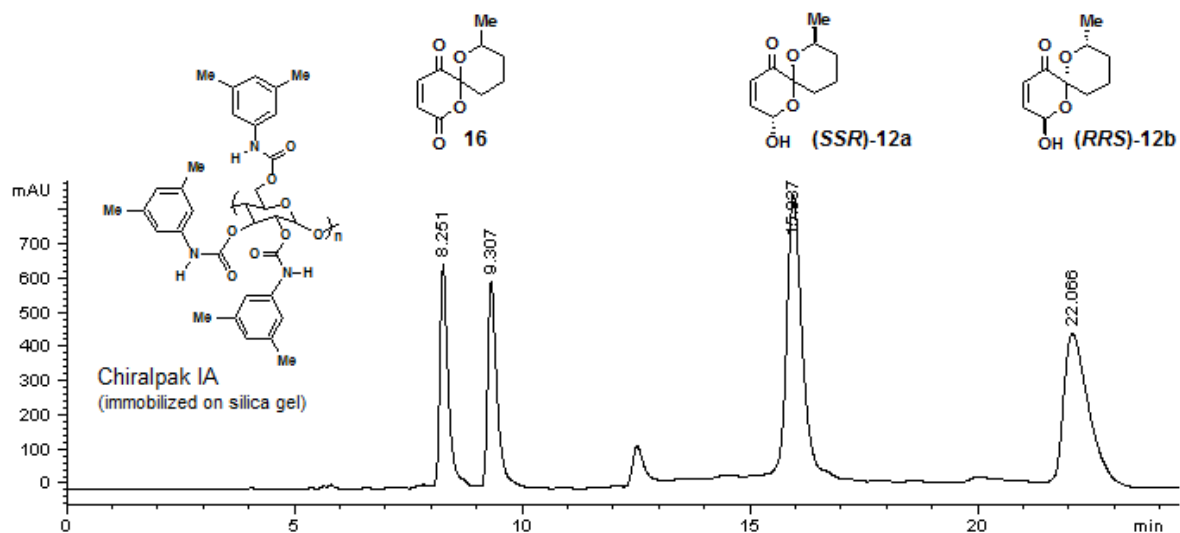


Figure 4. HPLC separation on Chiralpak IA

Each peak recovered by using Chiralcel OD-H was characterized by NMR spectroscopy. The NMR spectra of compounds eluted at 9.16 and 9.58 min (Table 1) allowed the identification of compound **16** probably derived by on-column rearrangement of **12**, whereas it was possible to assign the signals of compounds eluted at 11.24 and 12.23 min to the couple **12a** (*2S,6S,8R*) and **12b** (*2R,6R,8S*) (Figure 5).

Table 1. HPLC of stereoisomeric mixture of **12a-d** by using hex/IPA 95:5 as mobile phase at *FR* 0.8 ml/min.

Compound	Chiral Column							
	Chiralcel OD-H				Chiralpak IA			
	<i>t</i> [min]	<i>k</i>	α	R_s	<i>t</i> [min]	<i>k</i>	α	R_s
16	9.16	1.54	1.08	0.7	8.25	1.17	1.23	1.7
	9.58	1.66			9.31	1.44		
12a	11.24	2.12	1.13	1.2	15.94	3.19	1.51	5.7
12b	12.23	2.40			22.01	4.81		

However, **12** showed low on-column stability and this fact limited the recovery yield. Indeed, the injection of 28.0 mg of isomeric mixture on Chiralcel OD-H produced 3.9 mg of **12a** and 3.3 mg of **12b** (>99% e.e., 26% yield), whereas 45.6 mg of isomeric mixture produced 5.6 mg of each enantiomer, namely **12a** and **12b** (>99% e.e., 25% yield) on Chiralpak IA. To increase throughput, the technique of boxcar injections was used for all recoveries. The minor diastereoisomeric couple **12c,d** was not detected by HPLC analysis probably because of the low on column stability of the spiroketal **12**. The enantiomer elution order was determined by injection of a sample of diastereomeric mixture **12a,c** obtained from the enantiopure (*R*)- δ -hexalactone **14** (Scheme 1).

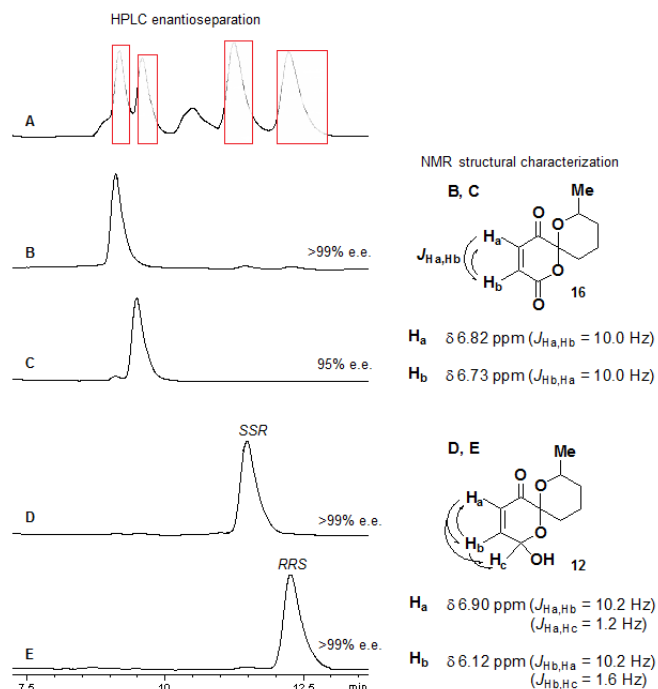


Figure 5. NMR structural characterization of compounds recovered by means of chiral HPLC on Chiralcel OD-H.

Biology.

Anti-proliferative activity of spiroketals stereoisomeric mixture **12a-d**

First, biological studies on the stereoisomeric mixture of **12a-d** have been carried out using representative human tumor cell lines with different histological origin: MCF-7 breast carcinoma, M14 melanoma, H125 pulmonary carcinoma, HT-29 colon carcinoma, HL-60 promyelocytic leukemia and SH-SY5Y neuroblastoma. The tumor cell growth has been evaluated by counting viable cells number by a trypan blue dye exclusion test. The results, illustrated in Figure 6 in terms of viable cell number, showed that spiroketal stereoisomeric mixture **12a-d** used at different concentrations (7.8 nM, 15,6 nM 31.2 nM, 62.5 nM , 125 nM 250 nM), for culture times from 24 to 72 hours, induce a remarkable inhibition of cell proliferation. The cell growth inhibition was observed in all treated tumor cells and is time and dose correlated. In particular, the treatment with

250nM of stereoisomeric mixture (**12a-d**) induced a potent cytotoxic effect in all lines, since, more than 90% of treated tumor cells were found to be dead as early as 24 h after treatment.

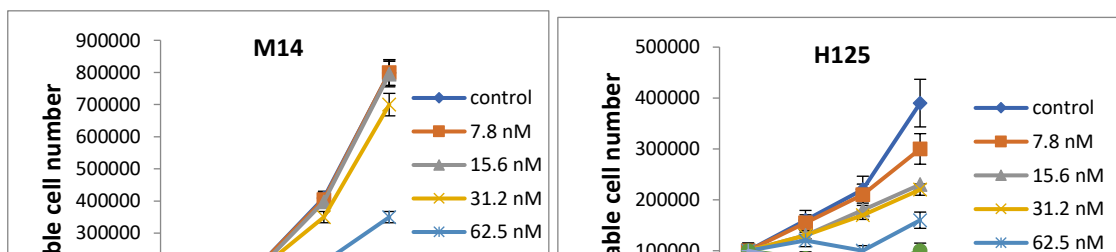


Figure 6. The antiproliferative effect of the stereoisomeric mixture of **12a-d** on human tumor cell lines: M14 melanoma, H125 pulmonary carcinoma, HL-60 promyelocytic leukemia, HT-29 colon carcinoma, MCF-7 breast carcinoma, and *SH-SY5Y* neuroblastoma cell line. Cell growth kinetics was evaluated in terms of number of viable cells. The cell proliferation, viability and death have been determined by means of cell counts in trypan blue (dye exclusion test). Data are expressed in terms of number of viable cells. Measurements were done in triplicate, bars represent \pm SE of the

mean of three wells. Values are referred to a representative experiment, from least three independent experiments.

Anti-proliferative activity of enantiomerically pure enantiomers **12a and **12b****

The evaluation of anti-proliferative effects has been also carried out using the enantiomerically pure enantiomers **12a** (2*S*,6*S*,8*R*) and **12b** (2*R*,6*R*,8*S*) obtained *via* chiral HPLC separation. The tumor cell line M14 (human melanoma) has been used as representative tumor cell line to compare the anti-proliferative effectiveness of **12a** and **12b** with respect to the stereoisomeric mixture **12a-d**. Treatment was performed with serial concentrations of **12a**, **12b** and the racemic mixture of stereoisomers **12a-d** as reference compound from 62.5 nM to 250 nM (12.5, 25, 50, µg/mL) at culture times varying from 24 to 72 hours. The effect of **12a**, **12b** and **12a-d** on cell proliferation of melanoma cell line M14 was determined by cell counts in trypan blue (dye exclusion test) using a hemocytometer (see below). Cell proliferation results show that treatment with enantiopure **12a**, **12b** and **12a-d** stereoisomeric mixture at different concentrations always induce in M14 cell line a remarkable inhibition of cell proliferation, depending on culture time and concentration (Figure 7). In addition, as showed in Figure 8, taking a reference dose 250 nM, the tumor growth inhibition is comparable for both enantiomers and the stereoisomeric mixture in M14 line by using a CellTiter 96[®] Non-Radioactive Cell Proliferation. The results are referred to optical density (OD). Taking together the results showed, a comparable effect of enantiomers **12a** and **12b** and the stereoisomeric mixture **12a-d** in inhibiting M14 cell growth. The inhibition activity of both enantiomers and the stereoisomeric mixture on M14 cell grow is also substantially comparable when evaluated in terms of kinetic cell growth.

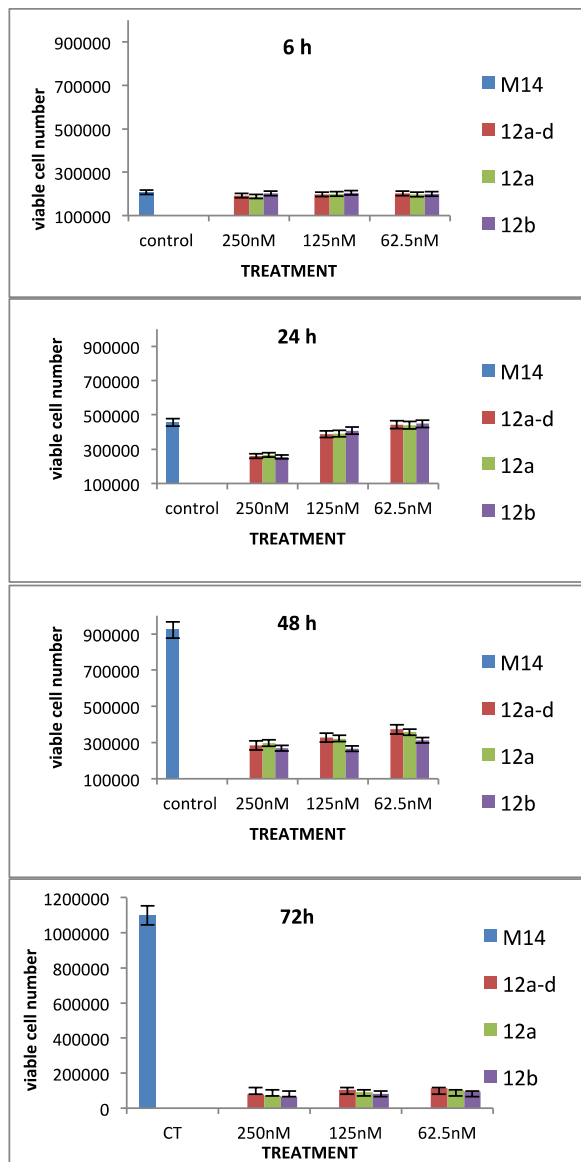


Figure 7. Effect of pure enantiomers **12a** and **12b** and stereoisomeric mixture **12a-d** on tumor cell growth of M14 melanoma cell line. Cells were cultured in complete medium containing the indicated concentrations of **12a**, **12b** and **12a-d**, for 6, 24, 48 and 72 h. Control groups were treated with DMSO alone. Cell proliferation was determined by trypan blue dye exclusion assay. Data are expressed in terms of viable cells number. Measurements were done in triplicate. Values of a representative experiment, from at least three independent experiments, represent the mean \pm SE of three wells.

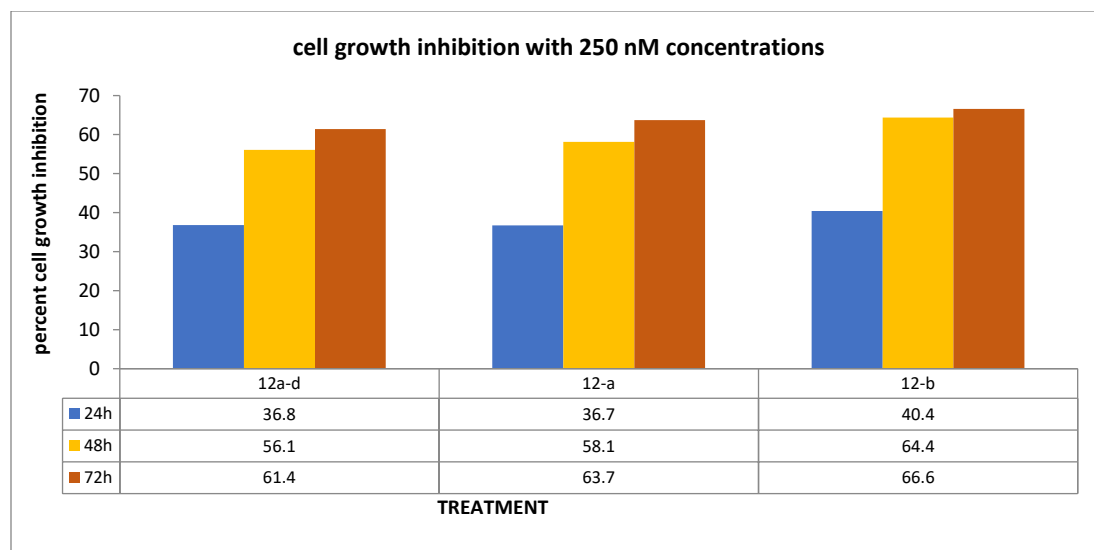


Figure 8. Effect of 250nM of pure enantiomers **12a** and **12b** and stereoisomeric mixture **12a-d** on tumor cell growth of M14 melanoma cell line evaluated at 24, 48 and 72 h. Cell proliferation was determined by CellTiter 96® Non-Radioactive Cell Proliferation. Measurements of optical density (OD) were done in triplicate in three different experiments. Data are expressed in terms of percentage of cell growth inhibition with respect to control.

Proapoptotic in vitro activity

The role of apoptosis in the origin of the inhibitory effect of **12a-d** on cell proliferation has been previously investigated by flow cytometry.²⁴ In order to confirm this proapoptotic effect of **12a-d**, the activation of caspases 3/7, which are mediators of apoptosis, was analyzed upon exposure of SHSY5Y neuroblastoma cell line to the **12a-d** mixture. In order to avoid an excessive cytotoxicity the experiments were performed using very low doses (7.8 nM, 15.6 nM, 31.2 nM) of the **12a-d** mixture and for a relative short time, 24 h. The levels of caspase activation in SHSY5Y neuroblastoma cells were compared with untreated control cells arbitrarily set to 1.0. The results, expressed as caspase 3/7 activity fold increase showed that the **12a-d** significantly increase caspase

3/7 activation at different concentrations. At 31,2 nM, the caspase 3/7 activity reached a maximum, 8.2 fold increase at 24h (Figure 9).

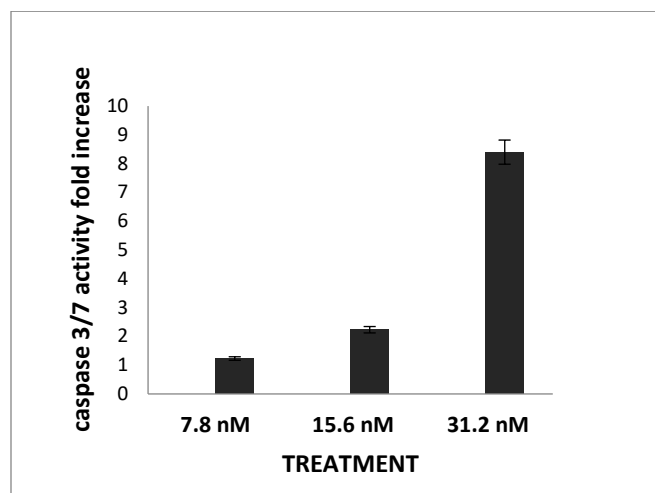


Figure 9. Apoptosis mediated by caspase3/7 activation. Treatment of cells with various concentration of **12a-d** for 24 h. The levels of caspase activation in SHSY5Y neuroblastoma cell line were compared with untreated control cells arbitrarily set to 1.0. Measurements were done in triplicate, bars represent \pm SE of the mean of three wells. Values are referred to a representative experiment, from at least three independent experiments.

Telomerase in vitro activity

In order to provide additional information on the antitumor effects of **12a-d** on malignant cells, experiments were performed to test the *in vitro* influence of the compound on Telomeric activity (TELMA), the enzyme strongly associated with cancer progression and cell immortalization.²⁸⁻³² MCF-7, H-125 HT-29 and M14 tumor cells were exposed in vitro to 31,2 nM to 250 nM of stereoisomeric mixture **12a-d**. After 48 hours of treatment TELMA was evaluated. In all examined cell lines a reduction of TELMA was observed as shown in Table 2. The results were expressed as percentage of inhibition with respect to untreated cell line. The inhibition is concentration-dependent in all lines examined. In particular M14 melanoma cell line appear as the

most sensible tumor line respect to TELMA inhibition reaching around the 62% of TELMA inhibition at the lower concentration of **12a-d** (31.2 nM). IC50 of **12a-d** ranging from 12,6 to 85,2 nM depending from the cell lines. To the best of our knowledge the spiroketal **12a-d** is one of the most potent telomerase inhibitor known.

Table 2. Dose-dependent percent of inhibition of TELMA, respect to untreated control obtained by stereoisomeric mixture **12a-d**.

TUMOR LINE	Percent of inhibition of TELMA by 12a-d after 48 h			
	31.2 nM	62.5 nM	125 nM	250 nM
MCF7 breast cancer cell	0	37.5	67.9	78.6
M14 melanoma	62	63	74	82.6
H125 lung carcinoma	13.6	48.7	67.6	75.7
HT29 colon carcinoma	24	53.5	69	73.4

TELMA was detected by telomeric repeat amplification protocol enzyme-linked immunosorbent assay after 48 h. The percent of inhibition was calculated between the means of treated versus untreated control, all experiments were done in triplicate.

Circular Dichroism Studies

Since a spiroketal telomerase inhibition effect could be a consequence from a stabilization of G4, CD spectroscopy was used to investigate the binding property of the spiroketal stereoisomeric mixture to telomeric G4.³³⁻³⁴ In order to investigate the influence of **12a-d** towards the G4 stability by a sequence taken from the human telomeric DNA, a 2.5 μ M solution of tel22 G4 has been incubated with 50 eq of **12a-d** in two buffer systems: 0.01 M Tris-HCl (pH 7.5), 0.2 M KCl and

PBS 1x (pH 7.5). The conformation adopted by tel22 G4, after annealing under the above described experimental conditions, is essentially identical to that observed by Hudson et al.³⁵, as confirmed by comparison of its CD spectrum with literature reports. Its stability has been analysed by CD-melting experiments, monitoring the CD signal changes at 295 nm registered upon increasing the temperature in the range 10 - 90 °C (Figure 10). G4 exhibits a T_m of 69 °C in 0.01 M Tris-HCl (pH 7.5), 0.2 M KCl. In contrast, the G4 was markedly less stable in PBS 1x (pH 7.5) exhibiting a T_m of 60 °C. After incubation with **12a-d**, CD-melting experiments (Figure 10) have been performed on the systems G4/12 in both the buffer systems, mixed in 1:50 ratio; these results show that **12a-d** does not affect the CD-melting curve of the G4.

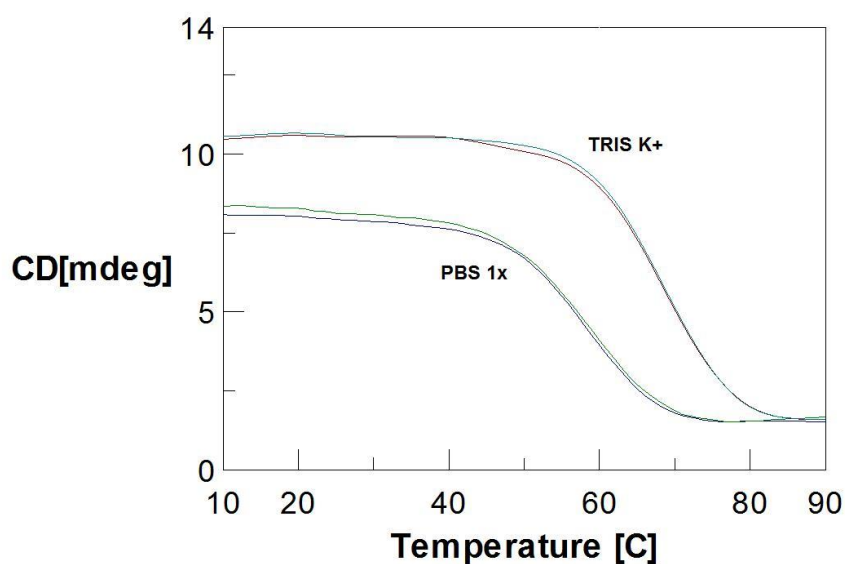


Figure 10. overlapped CD-melting curves of tel22 (2.5 μ M, PBS 1x, pH 7.5) in the absence (green line) and presence of 50 eq of **12a-d** (blue) and tel22 (2.5 μ M, 0.01 M Tris-HCl - 0.2 M KCl, pH 7.5) in the absence (cyan line) and presence of 50 eq of **12a-d** (red), recorded at 295 nm with a temperature increase of 1 °C/min;

Molecular Modeling

No crystallographic data of human telomerase is available, however a homology model was elaborated based on the *Tribolium castaneum* structure in the past.³⁶ Skordalakes and co-workers highlighted further structural conservative elements between human and *Tribolium castaneum* telomerase. A conserved and solvent-exposed hydrophobic pocket to accommodate small molecules is formed by the thumb domains of $\alpha 20$, $\alpha 21$, $\alpha 22$, and $\alpha 23$ helices present in both species telomerases.³⁷ We were docking the different spiroketal stereoisomers into the presumed binding site formed by the four α -helices. We used glide score to rank the poses of **12a-d** and glide emodel to fetch the best/worst ones. The ligand and the receptor site show nice shape and electrostatic complementarity. Our docking studies predicted several van der Waals interactions between the aliphatic moiety of the spiroketal scaffold and the hydrophobic residues Phe 482, Ile 556, Ile 550, Leu 554 and Phe 494 and hydrogen bonds between the hydroxyl, ether and carbonyl oxygens and Leu 554, Asp 493, Asn 492, Arg 486 and Tyr 551. Next we used scorpion analysis ranks ligand atoms individually in the context of cooperativity between a protein ligand complex to help understanding the network interactions (Figure 11).³⁸

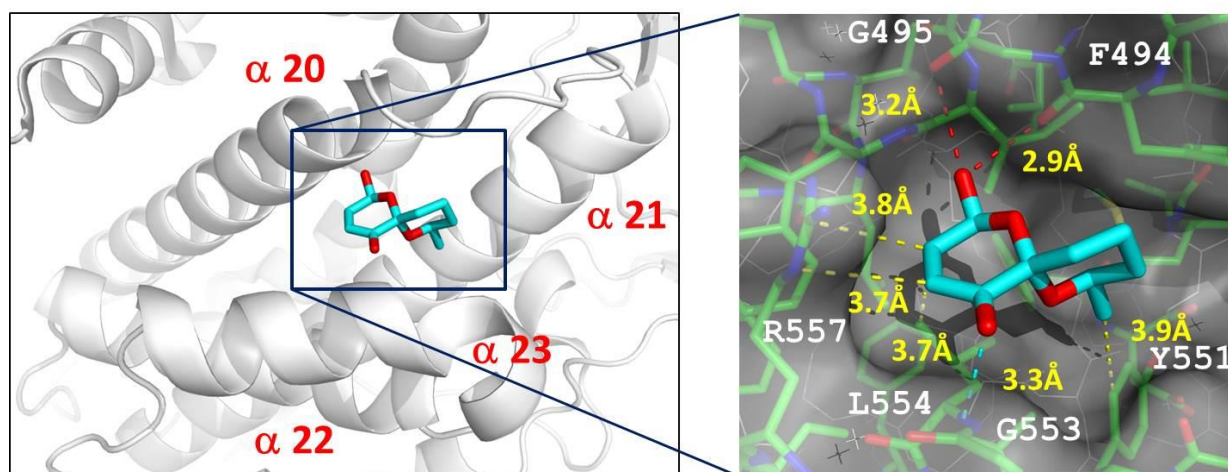


Figure 11. Modeling of spiroketal **12a** into the *Tribolium castaneum* topoisomerase (PDB ID 5CQG). Left: overview of the α -helical secondary structure around the binding pocket. Right:

close-up view of the binding site with the spirooxindole **12a** shown as cyan sticks and the receptor residues as green sticks. Van der Waals, hydrogen bonding and dipolar interactions are shown in yellow, red and cyan dotted lines, respectively. The binding distances are indicated in yellow. The picture was rendered with PyMol.

Scorpion analysis predicted **12a** and **b** as the strongest binder. An exemplary scorpion analysis of the highest scoring pose of **12a** is shown in Figure 11. The hydroxyl group makes a bifurcated hydrogen bonding with the amide carbonyls of Gly495 and Phe494. Plenty of hydrophobic contacts are formed between the double bond and the Arg557 and Leu554. The methyl group is buried deeply in the receptor pocket and shows a close contact to the m-carbon of Tyr551. The spiroketone carbonyl oxygen forms a dipolar interaction with the amide group of Gly553.

CONCLUSIONS

New structurally simplified spiroketal inspired to natural bioactive products have been synthesised. Their enantiomeric separation and characterization has been performed. The compounds have shown a high apoptosis induction and one of the most potent human telomerase inhibition activity known with also a very high anticancer activity. Cell proliferation results showed that the synthesised compounds always induce a remarkable inhibition of cell growth in all cell lines treated with spiroketals, depending on culture time and concentration. The inhibition activity of both enantiomers on cell grow is substantially comparable. These results confirm the previously proposed central role of spiroketals framework for telomerase inhibition activity. Furthermore, our CD melting experiments converge in showing that compound **12a-d** does not affect the G4 thermal stability as revealed on tel22 human telomeric DNA. Our findings suggest that the ability of compound **12a-d** to interfere with the telomerase activity is not due to any

stabilization of telomeric G4 structures but follows other mechanisms. Docking studies showed several interactions between the spiroketal scaffold in the active site of telomerase and predict enantiomers **12a** and **12b** as the strongest binder of this enzyme.

EXPERIMENTAL SECTION

1. General Chemistry. All reactions were carried out under a nitrogen atmosphere. Solvents were distilled and dried by standard methods. NMR spectra were recorded at room temperature, unless stated otherwise, using a 400 MHz, Varian Mercury spectrometer. Shifts have been recorded in ppm relative to CDCl₃ solvent residual peak. The following abbreviations have been used to explain the observed multiplicities: s, singlet; d, doublet; dd, doublet of doublets; ddd, doublet of doublets of doublets; t, triplet; td, triplet of doublets; m, multiplet; bs, broad singlet. All chemical reagents and solvents were purchased from commercial sources and used without further purification. Column chromatography was performed using 230–400 mesh silica gel. Thin-layer chromatography (TLC) was used to monitor progress of the reaction. The purity of the final compound **12a-d** was determined by C, H, N analysis and was in agreement with the proposed structures with purity $\geq 95\%$. The purity of final compounds **12a** and **12b** was determined by high performance liquid chromatography (HPLC) analysis, with the purity of compounds being higher than 95% and >99% of enantiomeric excess. HPLC instrument was a Agilent 1100 Series HPLC system [high-pressure binary gradient system equipped with a diode-array detector operating at multiple wavelengths (220, 254, 280, 360 nm), a 20 μ l sample loop and a thermostatted column compartment] using Chiralcel[®] OD-H or Chiralpak[®] IA operating as described in the chiral HPLC experimental section 2.

2-(Furan-2-yl)-6-methyltetrahydro-2H-pyran-2-ol (15): Butyllithium (16 mmol) and TMEDA (15.1 mmol) were added at 0 °C to a solution of furan **13** (15.1 mmol) in 20 mL of THF and the mixture was stirred at the same temperature for three hours. The solution was cooled at -78 °C and then δ -hexalactone **14** was added. The reaction mixture was stirred at -78 °C for one hour and

then quenched by adding 10 mL of a saturated aqueous solution of NH_4Cl . The mixture was extracted with Et_2O (3x20 mL) and CH_2Cl_2 (3x20 mL) and the organic layers were dried over Na_2SO_4 and filtered. The solvent was then evaporated at room temperature and the crude product was purified by flash chromatography (AcOEt/hexanes 2:1) to give compound **15** as a colorless oil in a 70% yield. ^1H NMR (400 MHz, CDCl_3) δ 7.57 (d, $J = 2.0$ Hz, 1H), 7.18 (d, $J = 3.6$ Hz, 1H), 6.52 (dd, $J = 3.6, 1.6$ Hz, 1H), 6.36 (bs, 1H, OH), 3.85-3.77 (m, 1H), 2.86 (t, $J = 7.2$ Hz, 2H), 1.87-1.75 (m, 2H), 1.54-1.48 (m, 2H), 1.20 (d, $J = 6.4$ Hz, 3H). ^{13}C NMR (100 MHz, CDCl_3) δ 189.6, 152.5, 146.2, 117.0, 112.1, 67.3, 38.5, 38.0, 23.3, 20.1. Anal. Calcd for $\text{C}_{10}\text{H}_{14}\text{O}_3$: C 65.91, H 7.74. Found: C 65.01, H 7.20.

2-Hydroxy-8-methyl-1,7-dioxaspiro[5.5]undec-3-en-5-one (12a-d): NBS (0.2 mmol) was added to a solution of **15** (0.1 mmol) in 5 mL of THF/ H_2O (4:1) at 0 °C. The mixture was stirred for 1.5 h at 0 °C, quenched with 5 mL of an aqueous solution of $\text{Na}_2\text{S}_2\text{O}_3$, neutralized by adding an aqueous solution of NaHCO_3 and extracted with CH_2Cl_2 (3x20 mL). The organic phase was separated, dried over Na_2SO_4 filtered, and the solvent was evaporated under reduced pressure. The crude product was purified by flash chromatography (AcOEt/ hexanes 2:1) to give **12a-d** as a colorless oil in a 95% yield. ^1H NMR (400 MHz, CDCl_3) δ 6.95 (dd, $J = 14.0, 3.6$ Hz, 1Ha), 6.90 (dd, $J = 10.2, 1.2$ Hz, 1Hb), 6.12 (dd, $J = 10.2, 1.6$ Hz, 1Hb), 6.11 (dd, $J = 10.4, 0.8$ Hz, 1Ha), 5.67 (d, $J = 9.2$ Hz, 1Hb), 5.46 (dd, $J = 11.6, 2.8$ Hz, 1Ha), 4.38-4.30 (m, 1Ha), 4.04-3.96 (m, 1Hb), 2.18-2.06 (m, 1Ha, 1Hb), 1.96-1.84 (m, 1Ha, 1Hb), 1.77-1.48 (m, 3Ha, 3Hb), 1.39-1.31 (m, 1Ha, 1Hb), 1.16 (d, $J = 6.0$ Hz, 3Hb), 1.13 (d, $J = 6.4$ Hz, 3Ha). ^{13}C NMR (100 MHz, CDCl_3) 190.2, 178.2, 148.1, 145.2, 126.5, 124.7, 88.0, 87.3, 70.3, 69.1, 35.0, 34.0, 31.9, 27.7, 27.0, 21.4, 19.8, 17.9. Anal. Calcd for $\text{C}_{10}\text{H}_{14}\text{O}_4$: C 60.59, H 7.12. Found: C 60.90, H 7.27.

2. Chiral HPLC

Instrument. An Agilent Technologies (Waldbronn, Germany) 1100 Series HPLC system [high-pressure binary gradient system equipped with a diode-array detector operating at multiple wavelengths (220, 254, 280, 360 nm), a 20 μ l sample loop and a thermostatted column compartment] was employed both for analytical enantioseparations and multimilligram recovery of the enantiomers. Data acquisition and analysis were carried out with Agilent Technologies ChemStation Version B.04.03 chromatographic data software. The UV absorbance is reported as milliabsorbance units (mAU).

Chromatography. Chiralcel[®] OD-H (cellulose *tris*-3,5-dimethylphenylcarbamate) (Daicel, Japan) and Chiralpak[®] IA (amylose *tris*-3,5-dimethylphenylcarbamate) (Chiral Technologies Europe, Ilkirch, France) were used as analytical chiral columns (250 x 4.6 mm, 5 μ m). HPLC-grade *n*-hexane (hex) and 2-propanol (IPA) were purchased from Sigma-Aldrich (Taufkirchen, Germany). Analyses were performed in isocratic mode. The retention factor (k) was determined as $k = (t_R - t_0)/t_0$, where t_R is the retention time for the eluted enantiomer: k_1 is the retention factor of the first-eluted enantiomer. The separation factor (α) was calculated as $\alpha = k_2/k_1$. The resolution (R_s) was determined as $2(t_{R2} - t_{R1})/(W_1 + W_2)$ where W is the basewidth of peak. Dead time ($t_0 = 3.6$ min (OD-H), 3.8 min (IA)) was measured by injection of tri-*tert*-butylbenzene (Sigma-Aldrich, Germany) as a non-retained compound at flow rate (FR) = 0.8 ml/min.³⁹ For analytical runs, sample solutions were prepared by dissolving analytes in hex/IPA 1:1 (1.0-2.0 mg/ml). For multimilligram enantioseparations, the feed concentration of sample was 30 mg/ml (hex/IPA 1:1). Chromatographic separations were performed at 22°C.

3. Cell Proliferation Inhibition Assay

Cell lines

The study has been carried out using human tumor cell lines with different histological origin: MCF-7 breast carcinoma, M14 melanoma, H125 pulmonary carcinoma, HT-29 colon carcinoma, HL-60 promyelocytic leukemia. *SH-SY5Y* subline of the neuroblastoma cell line SK-N-SH. MCF7, H125, HT29 *SH-SY5Y* and HL60 were obtained from American Type Culture Collection (Rockville, MD). M14 (Golub et al., 1992), was kindly provided by Dr. G. Zupi (Istituto Regina Elena Rome, Italy). All cell lines were cultured at 37°C in 5% CO₂ humidified atmosphere and maintained in RPMI-1640 or DMEM F12 (Hyclone Europe, Cramlington, UK) supplemented with 10% heat-inactivated (56°C, 30 min) fetal calf serum (Hyclone Laboratories, Logan, UT), 2 mM L-glutamine, and antibiotics (Life Technologies Ltd., Paisley, Scotland) (referred to as complete medium, CM). Adherent cells were released from flasks by brief exposure to 0.025% trypsin with 0.01% EDTA.

Antiproliferative activity

Cell growth and viability was determined by trypan blue dye exclusion test. Cells were seeded in 24-well tissue culture plates (Falcon) at a concentration of 5×10^4 cells/mL and allowed to adhere overnight. Cells were incubated with **12a-d** (7.8 to 250 nM) or DMSO alone as control, 3 wells for each treatment. The plates were incubated at 37°C in a 5% CO₂ humidified atmosphere for 24, 48 or 72 h. Cell growth and viability were evaluated every 24 h. Trypsinized cells were manually counted using a hemocytometer and cell viability was determined by trypan blue dye exclusion assay.

The effect of **12a-d** or enantiomers **12a** and **12b** on cell proliferation of melanoma cell line M14 was determined by the CellTiter 96[®] Non-Radioactive Cell Proliferation (Promega Madison, WI, USA). Briefly, the cell suspension at an initial density of 8×10^4 cells/mL was seeded into 96-well plates and allowed to adhere overnight. Then, cells were treated with DMSO alone as control and

12a-d, 12a and **12b** (62.5, 125, 250 nM) for 6, 12, 24, 48 and 72 h. After treatment, the dye solution was added to the cell culture. Following incubation 4 h, the solubilization/stop solution was added to each well. The absorbance at wavelength of 570 nm was measured by an enzyme-linked immunoabsorbent assay reader. The negative control well contained medium only and was used as zeropoint of absorbance. The relative inhibition rate was calculated as a percentage, as follows: $(A \text{ control} - A \text{ experiment} / A \text{ control} - A \text{ negative control}) \times 100\%$.

4. Caspase-Glo® 3/7 assay

To confirm apoptosis induction, Caspase-3/7 activities were measured using Caspase-Glo® 3/7 assay kit (Promega, Madison, WI, USA) according to manufacturer's instructions⁴⁰ Briefly, tumor cells SHSY5Y were seeded in 96-well tissue culture plates (Falcon) at a concentration of 5×10^4 cells/ml and allowed to adhere overnight. After that the cells were exposed to of **12a-d** (7.8 to 31.2 nM) for 24 hours. The cells were incubated for 1 hour at 37°C with equal volume of Caspase-Glo® 3/7 reagent to the volume of culture medium. Adding the Caspase-Glo® 3/7 Reagent in an "add-mix-measure" format results in cell lysis, followed by caspase cleavage of the substrate. This liberates free aminoluciferin, which is consumed by the luciferase, generating a "glow-type" luminescent signal. The luminescence that is proportional to caspase 3/7 activities was determined by luminometer. A negative control consisting of cells treated with DMSO. supernatant containing **12a-d** alone was also included in each assay. The test was performed in triplicate.

5. Telomerase in vitro activity

In order to evaluate telomerase activity, MCF-7, H-125, M14 and H125 tumor cells were treated for 48 hours with serial doses of **12a-d** (from 31.2 to 250 nM) as described above. At the end of the treatment, the cells were harvested and washed twice with washing buffer and lysed in the lysis buffer. Supernatants were collected, rapidly frozen and stored at -80°C until the use. The

telomerase activity was determined using the TeloTAGGG telomerase PCR-ELISA plus Detection Kit according to the manufacturer's protocol (Roche Applied Science, Germany). Briefly, the cell extracts were incubated in presence of biotin-labeled primers for 30 min and the telomeric repeats were built by cell-extracted telomerase. Subsequently, the elongated products as well as especial internal standard were amplified by PCR and then, the PCR products were denatured and split in two aliquots and each separately hybridized to a digoxigenin-labeled detection specific probes and was then allowed to bind to a streptavidin coated 96-well plate and the biotin-labeled PCR products were detected using peroxidase-conjugated antibody. Finally, the absorbance of developed blue color was measured at 450 nm by an ELISA reader. The telomerase activity was measured in triplicate. As the negative control, each extract was heated at 95°C for 10 min prior to the PCR step. Relative telomerase activity (RTA) of each sample was calculated according to the instruction of TeloTAGGG Telomerase PCR-ELISA PLUS kit.

6. Circular Dichroism studies

Preparation of the ODN model system

The human telomeric sequence 5'-d(AGGGTTAGGGTTAGGGTTAGGG)-3' (Tel-22), was obtained from Eurofins Genomics (Ebersberg, Germany). DNA samples were prepared by dissolving the deoxyoligonucleotide in 0.01 M Tris-HCl (pH 7.5), 0.2 M KCl and PBS 1x (pH 7.5), followed by an annealing process in which the DNA solution was heated to 95 °C and slowly cooled to 4 °C over 12 hours. The formation of the G4 was confirmed at a concentration of 2.5 µM (strand) in a 1 cm path length cell using an Jasco J-810 spectropolarimeter: CD spectra in TRIS-K⁺ buffer showed a positive CD band centred at about 295 nm, which is characteristic of antiparallel G4 DNA structure, while in PBS 1X Tel-22 gave a CD spectrum compatible with that previously reported in the literature (Hudson et al. 2014).

CD-monitored melting experiments

For the CD melting experiments, the ellipticity has been recorded at 295 nm with a temperature scan rate of 1 °C/min in the range 10-90 °C. T_m values of 60 °C and 69 °C have been determined, respectively, for the G4 model systems in our two buffer conditions (0.01 M Tris-HCl (pH 7.5), 0.2 M KCl and PBS 1x (pH 7.5)). All the CD melting experiments have been performed in triplicate in a 1 cm path length cell at 2.5 μ M concentration of G4.

7. Docking studies

3D structures of **12a** and **12b** were generated using LigPrep, version 3.8 (Schrödinger, LLC, New York, NY, 2016) and Tribolium castaneum catalytic subunit of telomeras tcTERT in complex with highly specific BIBR1532 inhibitor (PDB ID: 5CQG) was prepared with protein preparation wizard. Grid receptor generation and docking studies were performed using Glide, while the receptor was kept rigid (version 7.1, Schrödinger, LLC, New York, NY, 2016).

Statistical analysis

Results means \pm SE. Statistical significance was determined using Student's t test.

Abbreviations Used

TELMA, Telomeric activity; OD optical density; G4, G-quadruplex; CD, circular dichroism; IPA, 2-propanol; ODN, oligonucleotide.

Corresponding Authors

*E-mail p.spanu@icb.cnr.it. Phone: +39 079 2841221

* E-mail mariapia.fuggetta@ift.cnr.it. Phone: +39 06 49934610

Funding Sources

This study was supported by Fase1 srl Viale Trento, 69 Cagliari - Italy

Notes

The authors declare no competing financial interest.

REFERENCES

- 1) Perron, F.; Albizati, K. F. Chemistry of Spiroketal. *Chem. Rev.* **1989**, *89*, 1617–1661.
- 2) Aho, J. E.; Pihko, P. M.; Rissa, T. K. Nonanomeric Spiroketal in Natural Products: Structures, Sources, and Synthetic Strategies. *Chem. Rev.* **2005**, *105*, 4406–4440 and references quoted therein.
- 3) Pettit, G. R.; Cichacz, Z. A.; Gao, F.; Herald, C. L.; Boyd, M. R.; Schmidt, J. M.; Hooper, J. N. A. Isolation and Structure of Spongistatin 1. *J. Org. Chem.* **1993**, *58*, 1302–1304.
- 4) Singh, S. B.; Zink, D. L.; Heimbach, B.; Genilloud, O.; Teran, A.; Silverman, K. C.; Lingham, R. B.; Felock, P.; Hazuda, D. J. Structure, Stereochemistry, and Biological Activity of Integramycin, a Novel Hexacyclic Natural Product Produced by *Actinoplanes* sp. that Inhibits HIV-1 Integrase. *Org. Lett.* **2002**, *4*, 1123-1126.
- 5) Takahashi, H.; Osada, H.; Koshino, H.; Kudo, T.; Amano, S.; Shimizu, S.; Yoshihama, M.; Isono, K. Reveromycins, new inhibitors of eukaryotic cell growth. I. Producing organism, fermentation, isolation and physico-chemical properties. *J. Antibiot.* **1992**, *45*, 1409-1413.
- 6) Takahashi, H.; Osada, H.; Koshino, H.; Sasaki, M.; Onose, R.; Nakakoshi, M.; Yoshihama, M.; Isono, K. Reveromycins, new inhibitors of eukaryotic cell growth. II. Biological activities. *J. Antibiot.* **1992**, *45*, 1414-1419.

- 7) Takahashi, H.; Yamashita, Y.; Takaoka, H.; Nakamura, J.; Yoshihama, M.; Osada, H. Inhibitory Action of Reveromycin A on TGF- α -dependent Growth of Ovarian Carcinoma BG-1 in vitro and in vivo. *Oncology Res.* **1997**, *9*, 7-11.
- 8) Cohen, P. The structure and regulation of protein phosphatases. *Ann. Rev. Biochem.* **1989**, *58*, 453-508.
- 9) Tachibana, K.; Scheuer, P. J.; Tsukitani, Y.; Kikuchi, H.; Van Engen, D.; Clardy, J.; Gopichand, Y.; Schmitz, F. J. Okadaic Acid, a Cytotoxic Polyether from Two Marine Sponges of the Genus *Halichondria*. *J. Am. Chem. Soc.* **1981**, *103*, 2469–2471.
- 10) Takai, A.; Murata, M.; Torigoe, K.; Isobe, M.; Mieskes, G.; Yasumoto, T. Inhibitory Effect of Okadaic Acid Derivatives on Protein Phosphatases. *Biochem. J.* **1992**, *284*, 539–544.
- 11) Marjanovic, J.; Kozmin, S. A. Spirofungin A: Stereoselective Synthesis and Inhibition of Isoleucyl-tRNA Synthetase. *Angew. Chem. Int. Ed. Engl.* **2007**, *46*, 8854–8857.
- 12) Ueno, T.; Takahashi, H.; Oda, M.; Mizunuma, M.; Yokoyama, a; Goto, Y.; Mizushima, Y.; Sakaguchi, K.; Hayashi, H. Inhibition of Human Telomerase by Rubromycins: Implication of Spiroketal System of the Compounds as an Active Moiety. *Biochemistry* **2000**, *39*, 5995–6002.
- 13) Chen, J. L.-Y.; Sperry, J.; Ip, N. Y.; Brimble, M. A. Natural Products Targeting Telomere Maintenance. *Med. Chem. Comm.* **2011**, *2*, 229-245.
- 14) Atkinson, D. J.; Brimble, M. A. Isolation, Biological Activity, Biosynthesis and Synthetic Studies towards the Rubromycin Family of Natural Products. *Nat. Prod. Rep.* **2015**, *32*, 811-840.
- 15) Mocellin, S.; Pooley, K. A.; Nitti, D. Telomerase and the Search for the End of Cancer. *Trends Mol. Med.* **2013**, *19*, 125–133.

- 16) Kiran, K. G.; Palaniswamy, M.; Angayarkanni, J. Human Telomerase Inhibitors from Microbial Source. *World J. Microbiol. Biotechnol.* **2015**, *31*, 1329–1341.
- 17) Rizvi, S. A.; Liu, S.; Chen, Z.; Skau, C.; Pytynia, M.; Kovar, D. R.; Chmura, S. J.; Kozmin, S. A. Rationally Simplified Bistramide Analog Reversibly Targets Actin Polymerization and Inhibits Cancer Progression in Vitro and in Vivo *J. Am. Chem. Soc.* **2010**, *132*, 7288–7290.
- 18) Kamachi, H.; Tanaka, K.; Yanagita, R. C.; Murakami, A.; Murakami, K.; Tokuda, H.; Suzuki, N.; Nakagawa, Y.; Irie, K. Structure–activity Studies on the Side Chain of a Simplified Analog of Aplysiatoxin (aplog-1) with anti-Proliferative Activity. *Bioorg. Med. Chem.* **2013**, *21*, 2695–2702.
- 19) Smith, A. B.; Risatti, C. A.; Atasoylu, O.; Bennett, C. S.; Tendyke, K.; Xu, Q. Design, Synthesis, and Biological Evaluation of EF- and ABEF- Analogues of (+)-Spongistatin 1 *Org. Lett.* **2010**, *12*, 1792–1795.
- 20) Uckun, F. M.; Mao, C.; Vassilev, O.; Huang, H.; Jan, S. T. Structure-Based Design of a Novel Synthetic Spiroketal Pyran as a Pharmacophore for the Marine Natural Product Spongistatin 1. *Bioorg. Med. Chem. Lett.* **2000**, *10*, 541–545.
- 21) Barun, O.; Kumar, K.; Sommer, S.; Langerak, A.; Mayer, T. U.; Müller, O.; Waldmann, H. Natural Product-Guided Synthesis of a Spiroacetal Collection Reveals Modulators of Tubulin Cytoskeleton Integrity. *Eur. J. Org. Chem.* **2005**, 4773–4788.
- 22) Mitsuhashi, S.; Shima, H.; Kawamura, T.; Kikuchi, K.; Oikawah, M.; Ichiharab, A.; Oikawa, H. The Spiroketal Containing a Benzyloxymethyl Moiety at C8 Position Showed the Most Potent Apoptosis-Inducing Activity *Bioorg. Med. Chem. Lett.* **1999**, *9*, 2007–2012.

- 23) Krohn, K.; Md. Sohrab, H.; Van Ree, T.; Draeger, S.; Schulz, B.; Antus, S.; Kurtán, T. Dinemasones A, B and C - New Bioactive Metabolites from the Endophytic Fungus *Dinemasporium strigosum*. *Eur. J. Org. Chem.*, **2008**, 5638–5646.
- 24) De Mico, A.; Cottarelli, A.; Fuggetta, M.; Lanzilli, G.; Tricarico, M. Dioxaspiroketal Derivatives, Process for their Preparation and Uses Thereof. WO/2007/132496, **2007**. US20100227919, **2010**.
- 25) Perron, F.; Albizati, K. F. Synthesis of Oxidized Spiroketal via 2-Furyl Ketone Oxidation-Rearrangement. *J. Org. Chem.* **1989**, 2044–2047.
- 26) De Haan, R. A.; Heeg, M. J.; Albizati, K. F. Synthesis of the Trioxa-Tricyclic Subunit of Saponaceolides via 2-Furyl Ketone Oxidation-Rearrangement. *J. Org. Chem.* **1993**, 291–293.
- 27) Aho, J. E.; Pihko, P. M.; Rissa, T. K. Nonanomeric Spiroketal in Natural Products: Structures, Sources, and Synthetic Strategies. *Chem. Rev.* **2005**, *105*, 4406–4440.
- 28) Fuggetta M.P.; Lanzilli, G.; Tricarico, M.; Cottarelli, A.; Falchetti, R.; Ravagnan, G.; Bonmassar, E. Effect of resveratrol on proliferation and telomerase activity of human colon cancer cells in vitro. *J. Exp. Clin. Cancer Res.* **2006**; *25*:189-93.
- 29) Lanzilli, G.; Fuggetta, M. P.; Tricarico, M.; Cottarelli, A.; Serafino, A.; Falchetti, R.; Ravagnan, G.; Turriziani, M.; Adamo, R.; Franzese, O.; Bonmassar, E. Resveratrol down-Regulates the Growth and Telomerase Activity of Breast Cancer Cells in Vitro. *Int. J. Oncol.* **2006**, *28*, 641–648.
- 30) Chen, C.-L.; Chang, D.-M.; Chen, T.-C.; Lee, C.-C.; Hsieh, H.-H.; Huang, F.-C.; Huang, K.-F.; Guh, J.-H.; Lin, J.-J.; Huang, H.-S. Structure-Based Design, Synthesis and Evaluation of

Novel anthra[1,2-D]imidazole-6,11-Dione Derivatives as Telomerase Inhibitors and Potential for Cancer Polypharmacology. *Eur. J. Med. Chem.* **2013**, *60*, 29–41.

31) Shirgahi Talari, F.; Bagherzadeh, K.; Golestanian, S.; Jarstfer, M.; Amanlou, M. Potent Human Telomerase Inhibitors: Molecular Dynamic Simulations, Multiple Pharmacophore-Based Virtual Screening, and Biochemical Assays. *J. Chem. Inf. Model.* **2015**, *55*, 2596–2610.

32) Ruden, M.; Puri, N. Novel Anticancer Therapeutics Targeting Telomerase. *Cancer Treat. Rev.* **2013**, *39*, 444–456.

33) Moye, A. L.; Porter, K. C.; Cohen, S. B.; Phan, T.; Zyner, K. G.; Sasaki, N.; Lovrecz, G. O.; Beck, J. L.; Bryan, T. M. Telomeric G-Quadruplexes Are a Substrate and Site of Localization for Human Telomerase. *Nat. Commun.* **2015**, *6*, 7643.

34) Ruden, M.; Puri, N. Novel Anticancer Therapeutics Targeting Telomerase. *Cancer Treat. Rev.* **2013**, *39*, 444–456.

35) Hudson J. S.; Ding L.; Le V.; Lewis E.; Graves D. Recognition and binding of human telomeric G-quadruplex DNA by unfolding protein 1. *Biochemistry* **2014**, *53*, 3347-56.

36) Steczkiewicz, K.; Zimmermann, M. T.; Kurcinski, M.; Lewis, B. A.; Dobbs, D.; Kloczkowski, A.; Jernigan, R. L.; Kolinski, A.; Ginalski, K. Human Telomerase Model Shows the Role of the TEN Domain in Advancing the Double Helix for the next Polymerization Step. *Proc. Natl. Acad. Sci.* **2011**, *108*, 9443–9448.

37) Bryan, C.; Rice, C.; Hoffman, H.; Harkisheimer, M.; Sweeney, M.; Skordalakes, E. Structural Basis of Telomerase Inhibition by the Highly Specific BIBR1532. *Struct. Lond. Engl. 1993* **2015**, *23*, 1934–1942.

38) Kuhn, B.; Fuchs, J. E.; Reutlinger, M.; Stahl, M.; Taylor, N. R. Rationalizing Tight Ligand Binding through Cooperative Interaction Networks. *J. Chem. Inf. Model.* **2011**, *51*, 3180–3198.

39) Koller, H.; Rimböck, K.-E.; Mannschreck, A. *J. Chromatogr. A* **1983**, *282*, 89-94

40) Chakravarti, B.; Maurya, R.; Siddiqui, J.A.; Bid. H. K.; Rajendran, S. M.; Yadav, P. P.; et al. In vitro anti-breast cancer activity of ethanolic extract of *Wrightia tormentosa*: role of pro-apoptotic effects of oleanolic acid and ursolic acid. *J. Ethnopharmacol.* **2012**; *142*, 72–9.

Table of Contents Graphic.

